KAWASAKI STEEL TECHNICAL REPORT
No.1 (September 1980)

Evaluation of Thermal Shock Resistance of Refractories by Using Acoustic Emission Technique

Masato Kumagai, Ryoji Uchimura, Hisashi Kishidaka

Synopsis :
Theoretical and experimental problems encountered in evaluating thermal shock resistance of refractories are summarized and a newly developed evaluation method using acoustic emission for detection of cracking is explained. It has been clarified that thermal shock conditions, specimen dimensions and restraining conditions, which were ignored in the previous studies, have a great influence on the thermal shock damage behavior. The evaluation based on the AE characteristics of refractories has a good correlation with actual service performance. Sufficient propriety for the evaluation is also given by the calculation of thermal stresses produced in a brick and the Hasselman's theory regarding the thermal shock damage.

The body can be viewed from the next page.

KAWASAKI STEEL TECHNICAL REPORT No. 1 September 1980

Evaluation of Thermal Shock Resistance of Refractories by Using Acoustic Emission Technique*

Masato KUMAGAI** Ryoji UCHIMURA**
Hisashi KISHIDAKA**

Theoretical and experimental problems encountered in evaluating thermal shock resistance of refractories are summarized and a newly developed evaluation method using acoustic emission for detection of cracking is explained.

It has been clarified that thermal shock conditions, specimen dimensions and restraining conditions, which were ignored in the previous studies, have a great influence on the thermal shock damage behavior. The evaluation based on the AE characteristics of refractories has a good correlation with actual service performance.

Sufficient propriety for the evaluation is also given by the calculation of thermal stresses produced in a brick and the Hasselman's theory regarding the thermal shock damage.

1 Preface

Refractories used in metal refining process often encounter spalling as they are subjected to severe temperature cycling. Spalling means cracking which leads to breaking away of refractories. It is a conspicuous example of thermal shock damage. Especially spalling damages at the hot spot of electric furnace[1], in LD converters and torpede cars[2,3] during preheating, and recently, at the bottom of bottom-blown converters[4] are well-known examples. Since thermal spalling leads to falling-off of brick fragments more than 10 mm long at a time, the adverse affect on refractory consumption as well as furnace operations is greater when compared with erosion or corrosion which shows relatively constant wearing rates. Because there has been no proper method for evaluating thermal shock resistance of refractories accurately before use, refractory selection and furnace pre-heating have been carried out empirically on a trial and error basis.

In this paper, the conventional theoretical and experimental evaluation methods of thermal shock resistance of refractories are summarized and a newly developed evaluation method using AE(acoustic emission) is described.

2 Conventional Studies on Thermal Shock Resistance of Refractories

2.1 Theoretical Evaluation

Generally, the materials behavior to thermal shocks is determined by the following factors[5]:

(1) Degree of thermal shock:
Degree of temperature change, conditions of heat trasfer between the material and surroundings
(2) Material properties:
Mechanical and thermal properties
(3) Geometric shapes of materials
(4) Degree of restraint:
Degree of restraining thermal expansion

Among these, (2) has been mainly studied because it is the factor to determine whether or not the material endures the thermal stress generated in it by a thermal shock, and it is also effective in comparing materials with respect to their properties and in determining the target properties for development or improvement. Especially, two main approaches have been made to evaluate the thermal shock resistance on the basis of materials property parameters.

The first approach treats crack initiation in the material by thermal stress. It is assumed that fracture occurs when the thermal stress generated inside the material exceeds the fracture stress (tensile stress in ceramics because they are much weaker in tension than under compression). The material property parameter

* Originally published in Kawasaki Steel Technical Report, 11 (1979) 1, pp. 132–143 (in Japanese)
** Research Laboratories

in this case is called thermal shock fracture resistance parameter, and various parameters are proposed according to the sample size and thermal shock conditions. Among these, following three equations assuming infinite flat plate by Kingery[6] are most generally used.

During rapid heating:

$$R = \frac{\sigma_f \cdot (1 - \nu)}{E\alpha} \quad \cdots\cdots (1)$$

During slow heating:

$$R' = \frac{\sigma_f \cdot k(1 - \nu)}{E\alpha} \quad \cdots\cdots (2)$$

During heating and colling at a constant rate:

$$R'' = \frac{\sigma_f \cdot k(1 - \nu)}{E \cdot \alpha \cdot \rho \cdot c} \quad \cdots\cdots (3)$$

σ_f : Fracture stress (tensile stress)
ν : Poisson's ratio
E : Modulus of elasticity
α : Thermal expansion coefficient
k : Thermal conductivity
ρ : Density
c : Specific heat

The second approach is based on the standpoint that avoids catastrofic crack propagation and is applicable to porous materials such as refractories. The material property parameter used in this case is called thermal shock damage resistance parameter. Two equations below are proposed by Hasselman[7].

$$R''' = \frac{E}{\sigma_f^2 \cdot (1 - \nu)} \quad \cdots\cdots (4)$$

$$R'''' = \frac{E \cdot \gamma}{\sigma_f^2 \cdot (1 - \nu)} \quad \cdots\cdots (5)$$

γ : Fracture surface energy

Equations **(4)** and **(5)** assume that the released strain energy during propagation of Griffith cracks equals the total surface energy of fracture. They are expressed using only material property terms and are reciprocally proportional to the surface area of the propagating crack. R''' is a convenient parameter assuming the same γ value among the materials compared and applicable to materials having relatively similar properties.

Hasselman[8] further proposed a theory to unify the thermal shock resistance parameters. Critical temperature difference ΔT_C for the initiation of crack propagation is given below on the assumption that disk-shaped Griffith cracks with a radius l exist uniformly at density N in the material and no interaction exists between them.

$$\Delta T_C = \left[\frac{\pi\gamma(1 - 2\nu)^2}{2E\alpha^2(1 - \nu^2)}\right]^{1/2} \times \left[1 + \frac{16(1 - \nu^2)Nl^3}{9(1 - 2\nu)}\right] l^{-1/2} \quad \cdots (6)$$

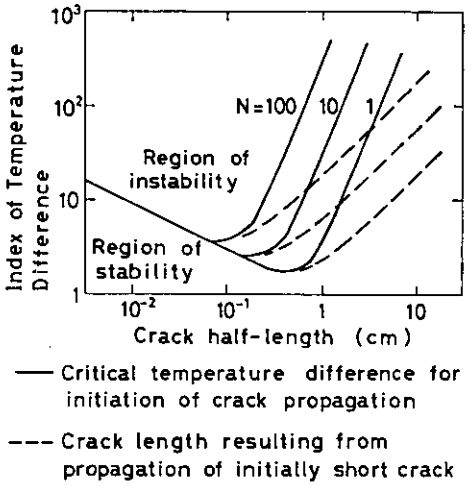

Fig. 1 Thermal stress crack stability and propagation behavior[8]

The relation of equation **(6)** is illustrated by the solid lines in **Fig. 1** for $\nu = 0.25$. On the left side of the minimum point of the solid line (when the initially existed cracks are short), crack propagation occurs when the temperature difference reaches ΔT_C. Since the initially existed cracks are short, the released elastic strain energy exceeds the fracture surface energy. So, the crack has a kinetic energy to propagate rapidly, finally reaching the crack length shown by the dashed lines. Fracture behavior in this state is catastrophic. It is called a dynamic fracture and corresponds to the thermal shock damage resistance parameter R''''. On the right side of the minimum point (when the initially existed cracks are long), on the other hand, cracks are expected to propagate in a stable manner. The fracture behavior is therefore quasi-static. Thermal shock damage resistance parameter for a quasi-static fracture is approximated assuming l value in equation **(6)** to be relatively large, and equation **(7)** is introduced using only the material property terms.

$$R_{st} = \left(\frac{\gamma}{E\alpha^2}\right)^{1/2} \quad \cdots\cdots (7)$$

The thermal shock damage resistance parameters expressed by using material property values as shown

above may be effective in providing target property values for material development and making comparison between materials. Depending on whether to require the resistance to crack initiation or to require the resistance to crack propagation, the evaluation result becomes contrary. In other words, E and σ_f in equations **(4)** and **(5)** are inverse to those in equations **(1)**, **(2)** and **(3)**, and E in equation **(7)** is inverse to that in equations **(4)** and **(5)**. These facts mean that the application of each equation will have an erroneous conclusion unless the fracture behavior under a certain termal shock condition is fully confirmed, and it is dangerous to evaluate only on the basis of the parameters. These theoretical evaluation methods do not provide the criterion to indicate whether a certain material is subject to dynamic fracture or quasi-static one. They are based on the over-simplified material models and thermal shock conditions. As a result, many difficulties follow the theoretical evaluation of thermal shock resistance of actual refractories. So, an experimental evaluation under conditions similar to actual thermal shock conditions is needed.

2.2 Experimental Evaluation

Various experimental methods for evaluating thermal shock resistance of ceramics and refractories have been proposed so far. Such methods classified according to the thermal shock conditions and detection methods of thermal shock damages are shown in **Table 1.**

Hasselman[9] and Nakayama[10] studied the radiation heating method for small rectangular bar specimens, paying attention to the correspondence with the theoretical evaluation. According to their results obtained for alumina-silica refractories, many specimens showed dynamic fracture under rapid heating conditions[9], and the critical temperature T_{rC} at which residual strength decreased discontinuously is related to R', and the fracture change in strength at T_{rC} is related to R''''[10]. Under rapid cooling conditions, all of the refractories exhibited quasi-static fracture behavior[9].

Table 1 Experimental methods for evaluating the thermal shock resistance of refractories

Thermal shock conditions	Detection of thermal shock damage
I) To the whole of specimen 1) Rapid heating 2) Rapid cooling a) Quenching by liquid b) Air cooling 3) Cyclic heating and cooling a) Cycles between $T_1 \leftrightarrow T_2$ b) Cycles using fluid media	I) Naked-eye inspection of cracks II) Residual strength III) Changes of Young's modulus
II) To a part of specimen 1) Heating or cooling at a constant rate 2) Cyclic heating and cooling	I) Naked-eye inspection of cracks II) Expansion by cracking III) Weight loss caused by peeling-off IV) Permeability V) Acoustic emission

DIN method is the most general among the test methods using relatively large specimens[11]. In this method, specimens 65 × 115 × 230 mm are generally used. The specimen is inserted to one third of its length into a furnace held at a given temperature, with the surface 65 × 115 mm as the leading end. The middle 1/3 is at the furnace wall and the rear 1/3 protrudes from the furnace. After being heated for a given time, it is taken out from the furnace and the heated portion is immersed into water. This cycle is repeated with visual observation of cracks and weight measurement excluding the spalled portion. The spalling resistance is evaluated by the number of cycles until 50 % of the heat portion falls off. Nakayama[12] confirmed good correspondence between the evaluation by this method and that by R'''' for alumina-silica refractories. Results obtained by such experimental evaluations are also strongly affected by thermal shock conditions and specimen dimension. So, proper evaluation of thermal shock resistance would be impossible unless the experimental conditions correspond to the actual service conditions. Sometimes, contradictions between experimental results and actual service performance have been experienced.

ASTM panel spalling method[13] is relatively similar to the actual service conditions of refractories. In this method, a wall constructed from refractories (panel) is heated and cooled to enable evaluation of spalling resistance by weighing the spalled fragments and observing the panel surface. Although it is a good method for simulating actual service conditions, it is not commonly used because of the lack of adequate damage detection method, the large scale of equipment and a long time needed. In addition, the results obtained are rather qualitative.

Recently AE measurement has been widely applied to the monitoring of fatigue and cracking of steel. A few applications of AE measurement to study thermal shock fracture of refractories have also been performed[5,14]. Under these environments, the authors have developed a new test method incorporating the panel method and AE measurement. It has been confirmed that by using this method good correlation can be obtained between the experimental results and the actual service performance for many kinds of refractories[15]. The merits of AE measurement as the detec-

tion method of crack initiation and propagation include the possibility of monitoring in real time, high sensitivity and high accuracy. On the other hand, there has been some demerits such as under-development in quantitative elucidation of AE mechanism and a difficulty in the calibration of the measurement system. In the following section, the authors will present these experimental results and discuss the capabilities of the evaluation for thermal shock resistance of refractories.

3 Thermal Stress Produced in Refractories during Experiment by Panel Method

It is important both for the study of thermal shock damage behavior and for determining experimental conditions to clarify the thermal stress distribution inside a refractory when a thermal shock is given by the panel method. There have been few studies about the thermal stress distribution in refractories when heated and cooled from one end, although a few qualitative discussions[16] have been made. Among them, the study about the relations between thermal shock and crack initiation by Kienow[2] is to be given special attention. Kienow analyzed thermal stress generated in magnesia refractories used for converters during heating at a constant rate, using a two-dimensional plane model, and derived the following relation on the assumption that a crack extends when the thermal stress exceeds the tensile stress of the refractory.

$$\frac{d^2T}{dx^2}\left(\frac{b^2}{16+3b^2/x^3}\right) \geqq \frac{\sigma_f}{E_\alpha} \quad \cdots\cdots\cdots (8)$$

b: Refractory width
x: Distance from hot face

He also demonstrated that the crack position corresponds to that predicted by equation (8).

Such thermo-elastical analytical calculation involves limitations due to calculation accuracy and complication in considering the effect of the size and external restraints. The authors, therefore, calculated the thermal stress distribution for magnesia-dolomite refractories using the finite element method. Details of the calculation are described in another report[17] and only the essentials related to the experiments are described here.

Thermal stress distribution which is produced in refractory heated from one end at a constant rate was calculated for a few temperature gradients during heating. Experimental temperature data shown in **Fig. 2** and **3** were used for the calculations. The results are shown in **Figs. 3, 4** and **5**. In **Fig. 3**, the normal stress component σ_x in x direction on the center axis becomes tensile as it goes further inward from the hot face. It reaches maximum at around 50 mm from the hot face and decreases gradually as the distance from

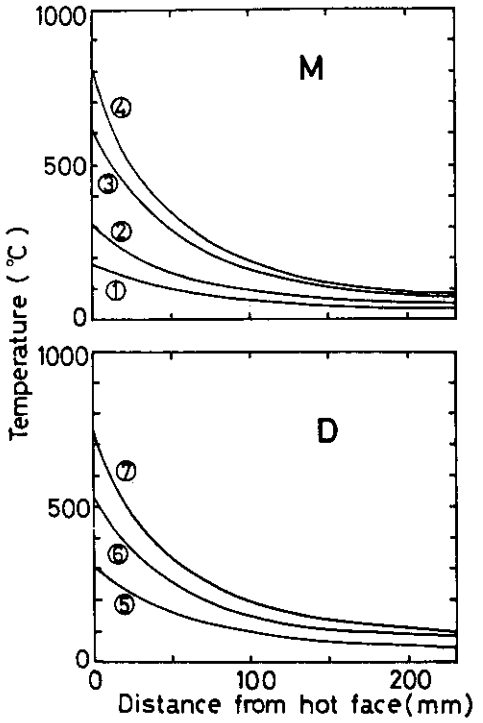

M: Magnesia-refractory
D: Magnesia-dolomite

Fig. 2 Temperature gradient in specimen for thermal stress analysis

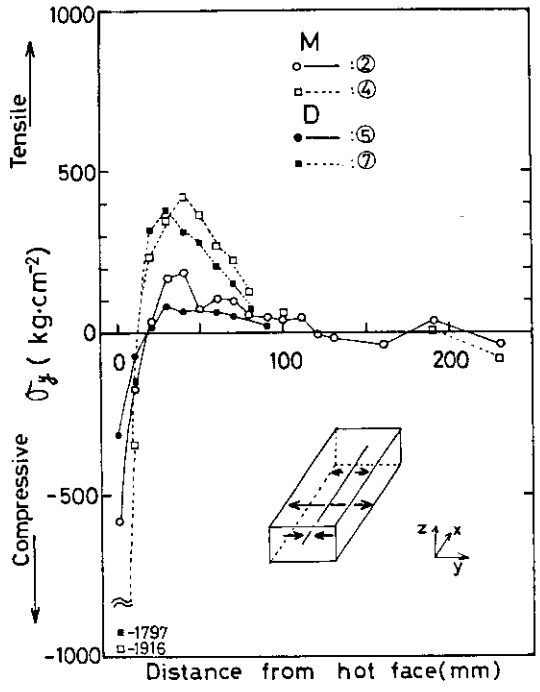

Fig. 3 Thermal stresses produced in refractory during heating from one end

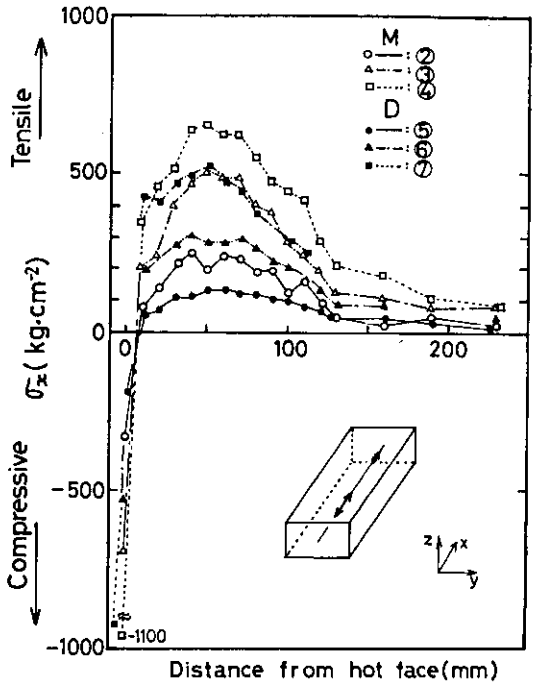

Fig. 4 Thermal stresses produced in refractory during heating from one end

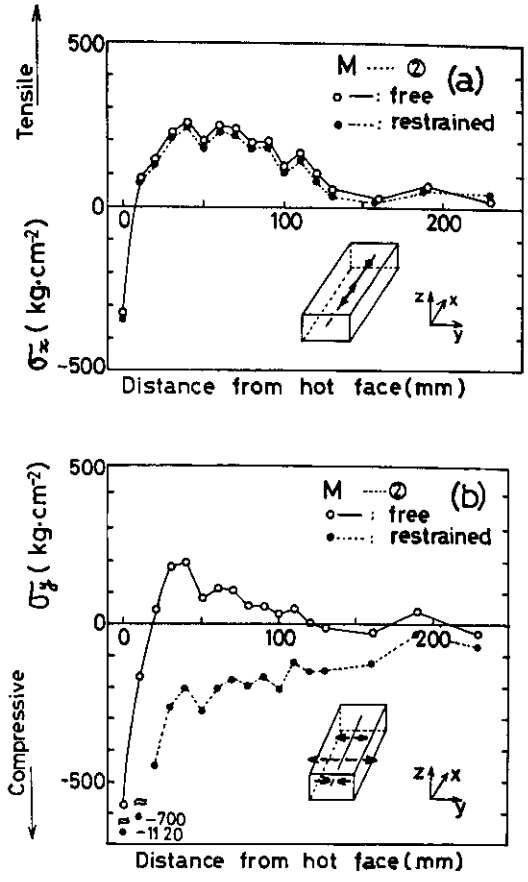

Fig. 5 Thermal stresses produced in refractory during heating from one end

the hot face increases further. Although σ_x increases with increasing temperature, comparative stress distribution remains almost unchanged. The normal stress component σ_y in y direction on the center axis, as shown in **Fig. 4**, shows almost the same trend as that of σ_x. But the absolute value of σ_y is smaller than that of σ_x and the position where σ_y reaches maximum is nearer to the hot face than that of σ_x. On the xy plane including the center axis, σ_x is tensile near the side surface (see **Fig. 5(a)**). On the same plane, around the center axis σ_y is compressive near the hot face and becomes tensile as it goes further inward. σ_y is approximately 0 near the side surface. (See **Fig. 5(b)**)

The bending strength values which can substitute the tensile ones as a matter of convenience are 215 kg/cm^2 for M and 119 kg/cm^2 for D. From the stress analysis, the following fracture process during heating is speculated. Fracture, at first, initiates near the center axis of refractory at about 50 mm inward from the hot face and propagates in the direction parallel to the hot face. Further heating causes cracking vertical to the hot face near the center axis.

Effects of specimen dimensions and external restraining conditions on the thermal stress are shown in **Figs. 6** and **7**. The change in σ_x along the center axis is shown in **Fig. 6** when the cross sectional area of the hot face is changed. As the cross sectional area increases and its shape approaches square, thermal stress increases with the maximum tensile region

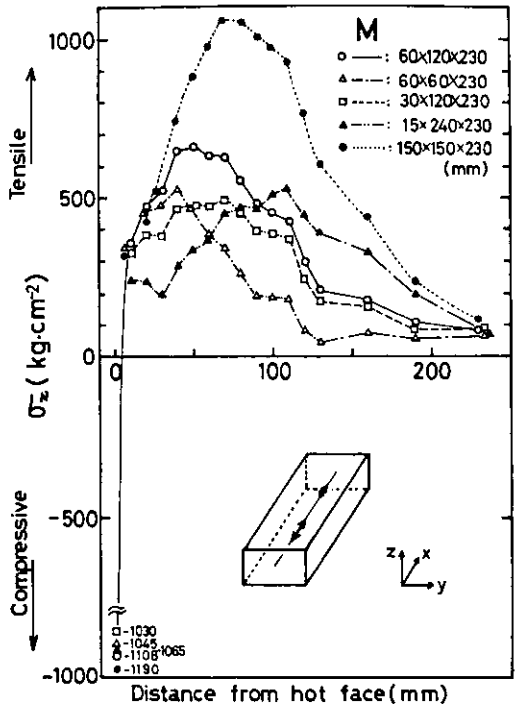

Fig. 6 Effect of specimen size on thermal stresses produced in refractory during heating from one end

moving away from the hot face. As shown in **Fig. 7**, the magnitude of σ_x is scarcely affected by the restraining stress in the direction parallel to the hot face. On the other hand, σ_y almost results in the super-position of the thermal stress component and the restraining stress.

Such effects of the specimen dimensions and external restraints on the thermal stress distribution are important in determining the experimental conditions. When the size is smaller, the thermal stress caused by the same thermal shock becomes smaller and crack initiation and propagation are different from those of a larger refractory. When the restraining stress is applied, cracks parallel to the hot face initiates as that in the case without restraining stress, but cracking vertical to the hot face is considered to be suppressed because σ_y is changed to the compressive side. The calculation here assumes the refractory to be a perfect elastic body and does not consider stress relaxation due to crack formation; so, it can not be said that the calculated stress distribution is perfectly the same as the thermal stress during a thermal shock experiment. However, as shown later, the calculation results correspond well to the experimental ones and provide powerful guide to a thermal shock experiment by the panel method.

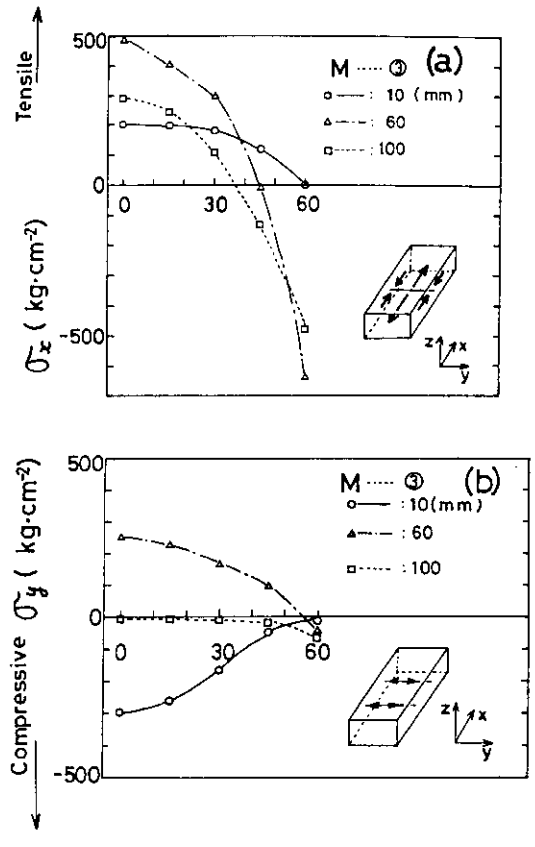

Fig. 7 Effect of restraining stress on thermal stresses produced in refractory during heating from one end

4 Evaluation of Thermal Shock Resistance Using AE Technique

The equipment for a spalling test by the panel method using AE technique is shown in **Fig. 8**. The refractory specimen installed in the panel is subjected to rapid heating and cooling by a heating furnace and a cooling fan. AE caused by crack formation in the refractory is detected by AE transducer which contacts the other side of the heated and cooled end via the stainless steel wave guide. Measurement of AE were carried out under the following condition:

Transducer: Single-ended and wide band type with center frequency 140 kHz fabricated from PZT
Pre-amplifier gain: 40 dB
Filter bandwidth: 0.1 ~ 1 MHz
Main amplifier gain: 30 dB

AE ringdown counts were derived by counter above 1 V threshhold. It has been confirmed that the measured AE characteristics correspond to crack initiation and propagation behavior in refractory[15]. In this experiment, the effects of heating rate, specimen dimension, restraining conditions and material properties on the thermal shock damage behavior, that is,

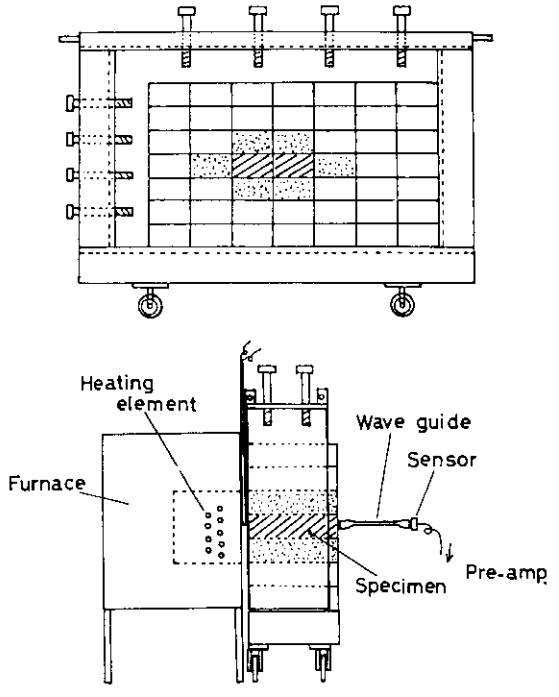

Fig. 8 Schematic illustration of panel spalling apparatus

Table 2 Typical properties of refractories

		Sample					
		M	D-1	D-4	A	MC-1	MC-2
Porosity (%)		13.8	15.0	13.9	16.4	14.9	14.8
Specific gravity		3.01	2.96	3.00	3.24	3.11	3.13
Compressive strength ($kg \cdot cm^{-2}$)		545	263	500	1580	562	640
Modulus of rupture S ($kg \cdot cm^{-2}$)	R.T.	215	119	104	310	65	162
	800°C	160	86	103	–	69	173
	1100°C	57	58	60	–	78	170
Modulus of elasticity E (10^4 $kg \cdot cm^{-2}$)		121	75	75	130	44	79
Chemical composition (wt %)	MgO	94	90.5	92.5	–	78.6	77
	CaO	0.8	8.1	6.5	–	0.7	0.50
	SiO_2	2.6	1.3*	0.91*	4.21	0.7	0.36
	Al_2O_3	0.6	–	–	92.3	4.9	6.35
	Cr_2O_3	–	–	–	2.81	9.3	12.3
	Fe_2O_3	0.5	–	–	–	3.3	3.41

* $SiO_2 + Al_2O_3 + Fe_2O_3$

on AE characteristics were studied. Finally, the possibility of evaluating thermal shock resistance of refractories is discussed. Typical properties of various refractories used in this experiment are shown in **Table 2**.

4.1 Heating Rate

Thermal shock was given by raising the furnace temperature at a constant rate. Relations between the total ringdown counts and hot face temperature for M and D-1 are shown in **Figs. 9** and **10**, respectively. For magnesia refractory M, a sharp increase of the total ringdown count was observed at the hot face temperature of around 920 °C in the case of heating rate of 2.2 °C/min. At higher temperatures, count rate was high but total count showed almost a continuous-like increase. As the heating rate increases, total ringdown count exhibited more and more a step-like increase but the absolute value of the total ringdown count became smaller. From the measurement results of the elastic modulus and residual strength after the thermal shock, an increase in the degree of damage in proportion to the increase of the heating rate has been confirmed[18].

On the other hand, no sharp increase in the ringdown count for all of the heating rates tested was observed for magnesia-dolomite refractory D-1. Except for a very fast heating rate range, total ringdown count was scarcely affected by the heating rate. From the ringdown count per unit time and observation of the AE waveform on the oscilloscope, the increase of the count rate and the AE wave amplitude

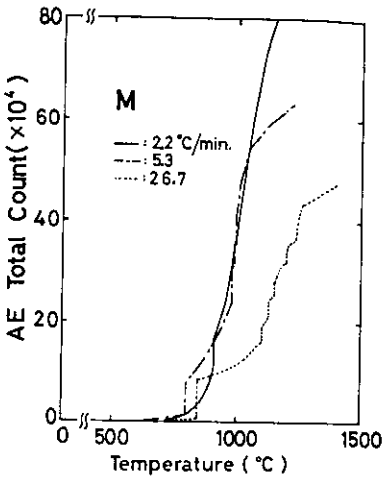

Fig. 9 Total ringdown count versus hot face temperature for magnesia refractory M during heating at different heating rates

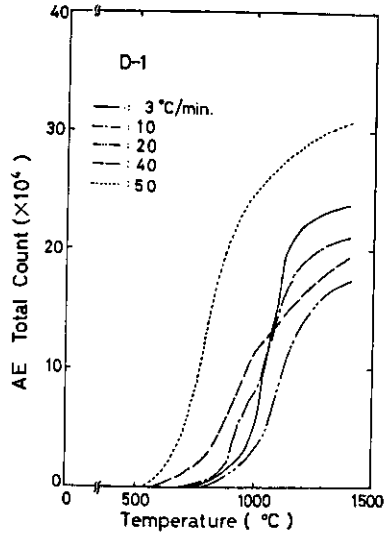

Fig. 10 Total ringdown count versus hot face temperature during heating for magnesia-dolomite refractory D-1 at different heating rates

in proportion to the increase of the heating rate was observed. As the heating rate increased, the decrease of the elastic modulus and the strength after thermal shock became remarkable[8].

It is to be noted here that the crack propagation behavior of refractory M was affected by the difference of the thermal shock conditions, but that of refractory D-1 was not. This fact shows that the crack propagation depends not only on the material properties but also on the thermal shock conditions even for the same material. Hasselman, et al.[9] also pointed out the difference of the crack propagation behavior between rapid heating and rapid cooling conditions. The results here have confirmed that it may change even under rapid heating conditions. So, for some

materials, inconsistency between the thermal shock condition in actual service conditions and the experimental conditions in evaluating the thermal shock resistance may result in an incorrect decision. Application of the AE technique to the panel method has such merits as changeability of thermal shock conditions and capability of high sensitive monitoring of crack propagation behavior, and it gives a result with better correspondence with the actual service performance than conventional experimental evaluation methods.

4.2 Refractory Materials

AE characteristics of various materials at the heating rate of 20 °C/min are shown in **Fig. 11**. Each specimen material exhibited different AE characteristics corresponding to the difference in the thermal shock damage behavior. The capability of monitoring of the crack propagation behavior for each material is

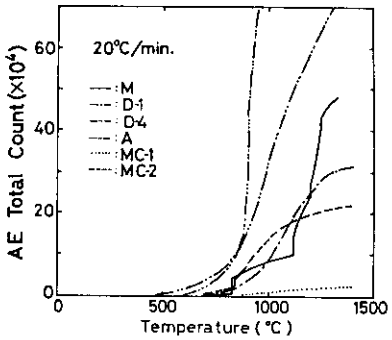

Fig. 11 Total ringdown count versus hot face temperature for various refractories

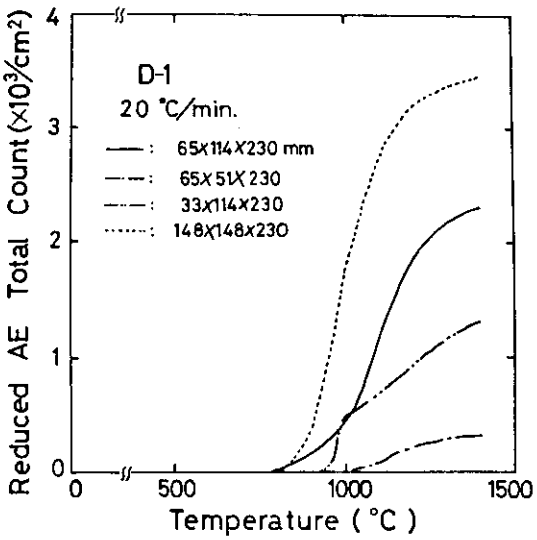

Fig. 12 Total ringdown count per unit cross sectional area parallel to the hot face versus hot face temperature at the rate of 10°C/min for various specimen sizes of magnesia-dolomite refractory D-1

effective in applying Hasselman's theoretical evaluation.

4.3 Specimen Size

Fig. 12 shows the test results for different cross sectional size of D-1 refractories. To eliminate the simple influence of the cross sectional area, the relation between the total ringdown count per unit cross sectional area and the hot face temperature is shown here. As the cross sectional area size decreases and the cross sectional shape approaches a square, the AE count and damage decrease. This result corresponds to the decreasing thermal stress for the specimen of smaller cross sectional area and the shape nearer to a square in thermal stress calculation.

At present when an absolutely quantitative measurement of AE is difficult, a perfection of quantitative discussion may be impossible but a quantitative grasping of the influence of specimen sizes on thermal shock damage is possible to a certain degree.

4.4 External Restraining Conditions

Fig. 13 shows the results of the M-1 refractory tests under different external restraining conditions. Strengthening of external restraints tends to decrease the total ringdown count, but the step-like characteristic becomes apparent. Different patterns were observed for different tests, but this may have been because the restraining conditions were not always constant. The

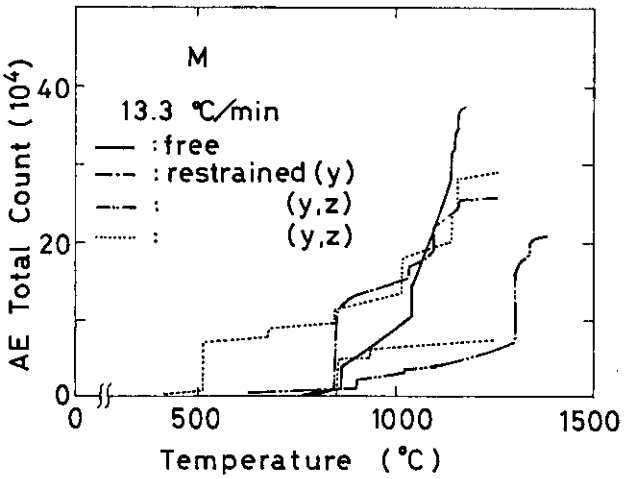

——— Free
— — — Restrained from expansion in y direction
— — — — Restrained from expansion in y and z direction
------- Compressed and restrained in y and z direction before testing

Fig. 13 Total ringdown count versus hot face temperature at the rate of 13.3°C/min for magnesia refractory M under different restraining conditions

step-like AE characteristic implies that the fracture proceeds in steps of unstable propagation—stop—unstable propagation. Since investigation of specimens after tests[18] shows a small decrease of elastic modulus in the direction of restraining stress and crack generation mostly in parallel planes to the hot face, the unstable propagation is considered to be occurring in a parallel plane to the hot face. This fact agrees with the thermal stress calculation result.

In actual use, refractories are seldom used individually but are used forming a curved or flat wall with other refractories. Therefore, thermal expansion is generally restrained externally. Under such conditions, crack propagation parallel to the hot face is encouraged more than during general thermal shock experiments. This point must be considered carefully when conducting a thermal shock experiment.

The fact that refractory sizes and restraining conditions affect the thermal shock damage means that not only refractory materials but the furnace constructing technique influences the thermal shock damage. Spalling damage may be decreased by reducing refractory size and relaxing external restraints.

4.5 Evaluation of Thermal Shock Resistance

As stated above, evaluation of different refractory materials simply on the basis of the ringdown count seems to involve problems because of the lack of the AE generating mechanism and the AE wave attenuation characteristic. Evaluation of refractories of the same material and with similar crack propagation patterns will be possible with a satisfactory result. The test results of magnesia-dolomite refractories of almost similar materials actually used for the lining of an LD convertor are explained below.

The sample refractories consist of 5 types, D-5 through D-9. **Table 3** shows the property values of each type. According to the spalling tests conforming to the DIN standard carried out by the refractory manufacturer, the spalling resistance was a little lower for D-7 while all other types were judged to have similar spalling resistance. **Fig. 14** shows the results of the tests by the panel-AE method for these refractories at the heating rate of 20 °C/min. In magnesia-dolomite refractories, the behavior of crack propagation by thermal shocks is all stable. In such a case, the degree of damage may be considered to correspond to the total ringdown count. With regard to the thermal shock resistance, D-9 and D-6 are much superior, followed by D-5 and D-8, and D-7 is considered to be the most inferior. With respect to the spalling damage during preheating of a convertor, D-7 showed spalling of about 20 t, D-5 and D-8 more than 10 t each, and D-6 and D-9 almost none. The panel-AE method provides the thermal shock conditions with good correspondence to actual service conditions and detects damage by the ringdown count, which is much more sensitive than visual observation. That is why this method gives such a good evaluation. Because the crack propagation is stable in these refractories, the relation between thermal shock parameter R_{st} during stable crack propagation and total ringdown count has been studied.

Table 3 Typical properties of refractories

		Sample				
		D-5	D-6	D-7	D-8	D-9
Porosity (%)		15.1	13.6	12.0	14.4	15.0
Specific gravity		2.95	2.96	3.08	2.96	2.96
Modulus of rupture S (kg/cm²)	R.T.	113	123	120	153	158
	800°C	139	182	142	154	186
	1100°C	83	98	62	86	82
	1400°C	36	67	25	46	48
Modulus of elasticity E R.T. (10^4 kg/cm²)		75	83	102	97	85
Fracture energy γ_{WOF} (10^4 erg/cm²)			10.8	7.2	11.5	11.4
$\sqrt{\gamma_{WOF}/E}$ ($\propto R_{st}$) (×10^{-2} cm$^{1/2}$)			3.64	2.68	3.48	3.70
Chemical composition (wt %)	MgO	91.5	90.5	90.5	87.0	87.0
	CaO	6.5	8.1	8.1	11.0	11.0
	SiO_2 + Al_2O_3 + Fe_2O_3	1.0	1.3	1.3	2.0	2.0

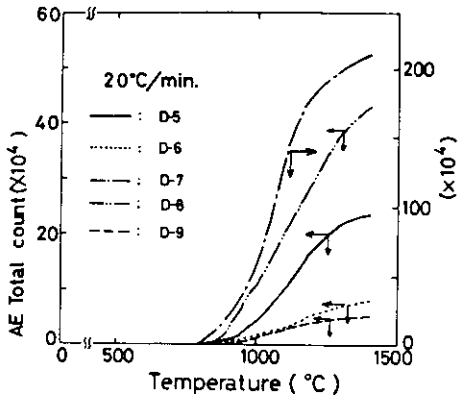

Fig. 14 Total ringdown count versus hot face temperature for five magnesia-dolomite refractories

Fig. 15 shows the relations between $R_{st} \propto (\gamma_{WOF}/E)^{1/2}$ and the total ringdown count assuming the same thermal expansion coefficient in magnesia-dolomite refractories. (γ_{WOF}: Fracture surface energy obtained by the work of the fracture method). A good correlation was observed between these, justi-

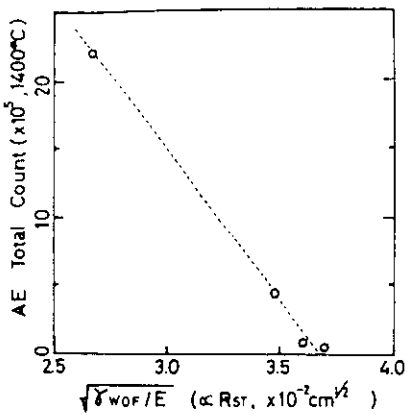

Fig. 15 Relation between total ringdown count and thermal shock damage resistance parameter

fying evaluation of thermal shock resistance during stable crack propagation on the basis of the ringdown count.

For materials involving unstable crack propagation, simple evaluation by the total ringdown count is difficult. If studies of the experimental method and data gathering proceed, with attention paid to the fact that AE characteristics change for the same material, depending on the thermal shock conditions and specimen sizes, then, the comparison between different materials will become possible.

5 Summary

This paper summarizes problems with theoretical and experimental evaluation of the thermal shock resistance of refractories and shows that the experimental method using the AE technique for detection of crack initiation and propagation is useful in evaluating the thermal shock resistance. Use of the AE technique enables monitoring of the crack propagation behavior of refractories, leading to the understanding of the differences of propagation behavior between different refractory materials, and the change of crack propagation behavior according to thermal shock conditions, specimen sizes and restraining conditions. This means the possibility of easy and accurate detection of the crack propagation behavior which is essential to theoretical evaluation. As a result, an advanced evaluation is possible as compared with the conventional experimental evaluation. The quantitative relationship between the degree of damage and the ringdown count is yet to be studied because of unknown factors in the AE generation mechanism and problems with AE measurement[19].

When viewed from a practical standpoint, evaluation of refractory materials with different crack propagation behavior or with apparent unstable crack propagation patterns is yet to be studied. However, evaluation of refractories with similar properties and with a similar propagation patterns is possible with satisfactory correspondence with evaluation based on actual use. Development of various evaluation methods, using AE based on study of testing conditions and data accumulation is expected in the future.

References

1) S.Kienow, K.Konopicky, et al.: Tonind. Z., **96** (1972) 10, pp. 306–312
2) S.Kienow: Ber.Deut. Keram. Ges., **47** (1970) 5, pp. 426–430
3) U.Fiedler, P.Jescheke, S.Kienow: Tonind.Z., **100** (1976) 5, pp. 181–189
4) K.Nakanishi, K.Sanbongi: Tetsu-to-Hagane, **65** (1979) 1, pp. 138–147
5) K.L.Leers, O.Schmidt: Tonind.Z., **100** (1976) 9, pp. 325–334
6) W.D. Kingery: J.Am. Ceram. Soc., **38** (1955) 1, pp. 3–15
7) D.P.H. Hasselman: ibid., **46** (1963) 11, pp. 535–540
8) D.P.H. Hasselman: ibid., **52** (1969) 11, pp. 600–604
9) D.R. Larson, D.P.H. Hasselman: Trans. J.Brit. Ceram. Soc., **74** (1975) 1, pp. 59–65
10) J.Nakayama: Fracture Mechanics of Ceramics, **2** (1973) (ed. E.R. Bradt, et al.), pp. 759–778 [Plenum Press]
11) DIN-51068
12) J.Nakayama: J.Am. Ceram. Soc., **48** (1965) 11, pp. 583–587
13) ASTM C 38–68
14) A.G. Evans: Proc. Brit. Ceram. Soc., **25** (1975), pp. 217–237
15) M.Kumagai, R.Uchimura, T.Kawakami: JOURNAL OF THE CERAMIC SOCIEYT OF JAPAN, **87** (1979) 5, pp. 259–267
16) M.J. Greaves: Iron Steel Eng., (1966) 9, pp. 187–192
17) M.Kumagai, R.Uchimura, T.Kawakami: JOURNAL OF THE CERAMIC SOCIETY OF JAPAN, **87** (1979) 7, pp. 356–364
18) M.Kumagai, R.Uchimura, T.Kawakami: JOURNAL OF THE CERAMIC SOCIETY OF JAPAN, **87** (1979) 6, pp. 307–317
19) Ed.M.Onoe, et al.: Fundamentals and Applications of Acoustic Emission, (1977) [Corona Press] (in Japanese)